EFFECT OF THE BULK STRESS ON STRESSES PRODUCED BY CONTACT OF CYLINDERS UNDER PARTIAL SLIP

Marina Frossard Ribeiro Mendes.
University of Brasilia, Institute of Technology, Dpt. of Mechanical Engineering,
inafrossard@brturbo.com

José Alexander Araújo.
University of Brasilia, Institute of Technology, Dpt. of Mechanical Engineering, alex07@unb.br

Edgar Nobuo Mamiya.
University of Brasilia, Institute of Technology, Dpt. of Mechanical Engineering, mamiya@unb.br

Abstract. *The goal of this work is to describe the field of stresses produced by a mechanical configuration under fretting fatigue. Fretting fatigue is a particularly severe form of fatigue that occurs when a component is subjected to small amplitude oscillatory movements between contacting surfaces. This microslip may provoke the superficial ware of the component, accelerating the nucleation and early growing of cracks, which can lead to a premature failure of the component. This phenomenon usually happens on the presence of a bulk fatigue load, beyond the normal and tangential contact loads. The applied shear load is usually smaller than the limit for full sliding and a partial slip regime occurs at the contact interface. In this work we will verify the effect of this bulk stress on the stress field produced by the mechanical contact of cylinders under a partial slip regime.*

Keywords: *fretting fatigue, contact stresses, partial slip, bulk stress.*

1. INTRODUCTION

In the beginning of 20th century, the fretting phenomenon was first identified in specimens with crack on the claw region of fatigue machines (Eden *et al*., 1911). Later, Warlow-Davis (1941) observed that components under fretting conditions and cyclic load show a decrease of 13 to 17% in the endurance limit of the material.

Many engineering materials face applications in which the component is subjected to this conditions like, for example, in screwed and riveted joints, in couplings of shafts with gears or bearings, at the contacting surfaces of disks and blades in turbine engines or compressors, etc. Thus, the fail due to fretting fatigue, increase the frequency of maintenance intervals and the cost associated with the change of spare parts. In this setting, it is important that studies are carried out in order to develop tools or models which can predict more precisely the fretting fatigue strenght of mechanical components. The development of these models has been conducted, generally, considering the use of simpler contact configurations, where the variables involved on the fatigue phenomenon (like stress and strain) could be easily obtained and the conduction of validation tests is less expensive. Moreover, the stress field produced in these configurations is considered the driving force to the initiation and early propagation of fretting cracks, hence it is of utmost importance to quantify and vizulize such stress field. The main of this work is determine the

influence of bulk load over the stress field produced by the contact of cylinders under partial slip regime.

2. CONTACT OF CYLINDERS

2.1. Surface Tractions

The first step towards a solution for the subsurface stress field is to solve the contact problem itself, i.e., to find the magnitude and distribution of the surface tractions. A very wide range of plane contact problems may be solved by using two integral equations, which relate pressure distribution, *p(x)*, to normal displacement, *h(x)*, and shear traction, *q(x)*, to relative tangential displacement, *g(x)*. Again it should be emphasized this is a well defined technique and only the integral equations themselves will be shown followed by a summary of the solutions. Details concerning the derivation of such analysis may be found in Hills et al. (1993), and Johnson (1985). The integral equations for two elastically similar bodies are:

$$\frac{1}{A}\frac{\partial h}{\partial x} = \frac{1}{\pi}\int_{-a}^{a}\frac{p(\xi)d\xi}{x-\xi} \tag{1}$$

$$\frac{1}{A}\frac{\partial g}{\partial x} = \frac{1}{\pi}\int_{-a}^{a}\frac{q(\xi)d\xi}{x-\xi} \tag{2}$$

where A is the composite compliance defined as:

$$A = 2\left(\frac{\kappa+1}{4\mu}\right) \tag{3}$$

being κ=*3-4*ν in plane strain, ν is the Poisson's ratio and μ is the modulus of rigidity.

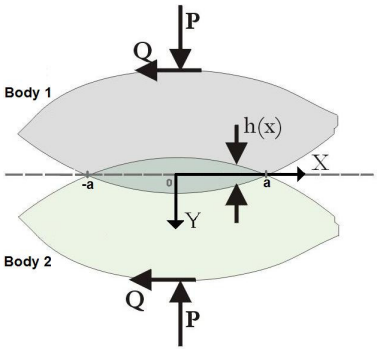

Figure 1: Contact between two elastically deformable bodies subject to a normal and shear force.

The configuration of interest in this work, which has been adopted to conduct a number of fretting fatigue tests by other researchers (Nowell, 1988, Araújo, 2000) is shown in Fig. (1). The pad radius, R and the normal load per unit thickness, P were defined so that each solid could be considered as an elastic half-space and the solution for the pressure distribution was Hertzian. The results of Hertz (1882) predict that due to a static normal force, an elliptical pressure distribution will develop:

$$p(x) = p_0 \sqrt{1 - \left(\frac{x}{a}\right)^2} \tag{4}$$

where p_o is the peak pressure and a is the semi-contact width

$$p_0 = \frac{2P}{\pi a} \tag{5}$$

$$a = \sqrt{\frac{4PR}{\pi E^*}} \tag{6}$$

where

$$R = \left(\frac{1}{R_1} + \frac{1}{R_2}\right)^{-1} \tag{7}$$

$$E^* = \left(\frac{1-\nu_1^2}{E_1} + \frac{1-\nu_2^2}{E_2}\right)^{-1} \tag{8}$$

where the subscripts 1 and 2 stand for body 1 (for instance, the fretting pad) and body 2 (tensile specimen).

The tangential load on the other hand will give rise to shear tractions as described by Mindlin (1949). Since in fretting fatigue tests, the applied shear load is usually smaller than the limit for full sliding, a partial slip regime develops where slip takes place within two symmetrical regions $c \leq |x| < a$ which surround a central stick region $|x| < c$. Therefore it seems convenient to model the shear tractions as a perturbation of the full sliding solution:

$$q(x) = fp_0 \sqrt{1 - \left(\frac{x}{a}\right)^2} - q'(x) \tag{9}$$

where the perturbation $q'(x)$ is zero in the slip zones $(c \leq |x| < a)$. In the stick region the shape of $q'(x)$ can be found by *(i)* recognizing there is no variation in the relative displacement between corresponding points $(g(x))$ in this region, and *(ii)* solving the integral equation given by Eq. (1) (Hills et al., 1993). Therefore,

$$q'(x) = 0 \qquad c \leq |x| < a \tag{10}$$

$$q'(x) = fp_0 \frac{c}{a} \sqrt{1 - \left(\frac{x}{c}\right)^2} \qquad |x| < c \tag{11}$$

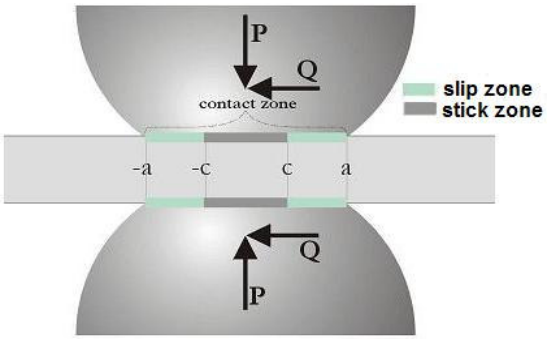

Figure 2: Stick and slip regions for the contact of cylinders in partial slip.

The size of the stick zone, c, is revealed by considering tangential equilibrium.

$$\frac{c}{a} = \sqrt{1 - \left(\frac{Q}{fP}\right)} \tag{12}$$

The expressions developed so far for the shear tractions are applicable only when the fretting force is at its extreme. To evaluate the tractions and consequently the stresses and/or strains at any other instant of the fretting cycle it is necessary to examine what happens to the reversal of the load. While such analysis has been carried out in detail elsewhere (e.g. Hills et al., 1993) an outline of the technique will be presented here.

To continue this analysis a recall of the boundary conditions within the stick and slip regions at the contact interface is advisable. For any point x within the slip zones the tractions are related by the well known Amonton's law.

$$\left|q(x)\right| = -fp(x) \tag{13}$$

Further, the direction of the shear tractions opposes the relative motion of the surfaces, yielding

$$\operatorname{sgn}(q(x)) = -\operatorname{sgn}\left(\frac{\partial g}{\partial t}\right) \tag{14}$$

where $\partial g/\partial t$ is the rate of change of the relative displacement $g(x)$. In the central region where there is no relative displacement between corresponding particles the shear tractions must be less than the limiting frictional value, thus:

$$\left|q(x)\right| < -fp(x) \tag{15}$$

Returning to the determination of the shear tractions, Fig. (3) depicts the variation of the tangential load with time. Increasing the load monotonically from 0 to Q_{max} point A is reached. At this stage Eq. (9) up to (11) were shown to describe the shear tractions. Now consider the load has been infinitesimally reduced from its maximum value to point B. This will cause a change of sign in the rate of change of the tangential displacement $\partial g/\partial t$, hence Eq. (14) will be violated and stick is expected in everywhere within the contact. Further, reducing the fretting load to point C will cause reverse slip at the contact edges. In these new slip zones ($d<|x|\leq a$) the shear traction will have

changed from $fp(x)$ to $-fp(x)$. Moreover, by analogy it is possible to infer that within the stick zones the corrective traction necessary to prevent slip will be given by:

$$q''(x) = +2fp_o \frac{d}{a}\sqrt{1-\left(\frac{x}{d}\right)^2} \tag{16}$$

Notice that the factor of two occurs because the corrective term must cancel the relative displacement occurring when the slip zone tractions change from $fp(x)$ to $-fp(x)$. The net shear traction at each particular region is therefore given as follows:

$q(x)/fp_o$	zone of application
$-\sqrt{1-\left(\frac{x}{a}\right)^2}$	$d < \lvert x\rvert \le a$
$-\sqrt{1-\left(\frac{x}{a}\right)^2} + 2\frac{d}{a}\sqrt{1-\left(\frac{x}{d}\right)^2}$	$c < \lvert x\rvert \le d$
$-\sqrt{1-\left(\frac{x}{a}\right)^2} + 2\frac{d}{a}\sqrt{1-\left(\frac{x}{d}\right)^2} - \frac{c}{a}\sqrt{1-\left(\frac{x}{c}\right)^2}$	$\lvert x\rvert \le c$

Table 1: Shear tractions for each region during variation of tangential load with time.

As with the case of monotonic loading the size of the new stick zone at the reversal of load is obtained from the overall equilibrium, yielding:

$$\frac{d}{a} = \sqrt{1-\left(\frac{Q_{\max} - Q}{2fP}\right)} \tag{17}$$

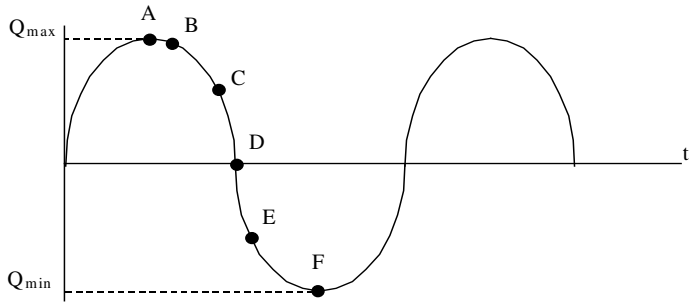

Figure 3: Variation of shear load Q with time t

Figure (4)a depicts the variation of shear tractions at different values of Q corresponding to points A, C, D, E and F of the fully reversed fretting cycle (Fig. (3)). It is worthy of notice that the shear tractions at extreme values of the tangential load (points A, Q_{max}, and F, Q_{min}) are equal and opposite. Moreover it is observed that after the total removal of the shear force (point D) non-zero but self-equilibrating shear tractions persist. This essentially means that frictional contacts are non-

linear and the shear traction distribution and consequently the stresses and strains in the contact bodies are history dependent. Therefore the application of the principle of superposition must be exercised with care in frictional contact problems.

If a moderate cyclic bulk load is applied in phase with the tangential load a time dependent offset of the stick zone, e (at maximum or minimum σ) or e' (during unloading or reloading), will be produced. Explicit expressions to work out the offset in the stick zone at any time of the loading cycle are given below. Again, no details concerning its derivation will be presented but a comprehensive development can be found in Hills et al. (1993).

$$\frac{e}{a} = \frac{\sigma_{\max}}{4fp_0} \tag{18}$$

$$\frac{e'}{a} = \frac{\sigma_{\max} - \sigma}{8fp_0} \tag{19}$$

Figure (4)b shows the history of shear tractions for a combination of bulk and shear loads similar to those applied in the Al series 1 experimental data by Nowell. The normalised bulk load σ/p_o varies between ± 0.59 in phase with the shear load, and its clear the shifting effect it produces on the shear traction distribution. Again it is necessary to say that the formulation developed above for the shifting of the stick zone is only valid for modest loads, which will produce $e+c$ and $e'+d<a$. For larger loads the size and position of the stick zone needs to be assessed numerically, for instance using quadratic programming (Nowell and Dai, 1998).

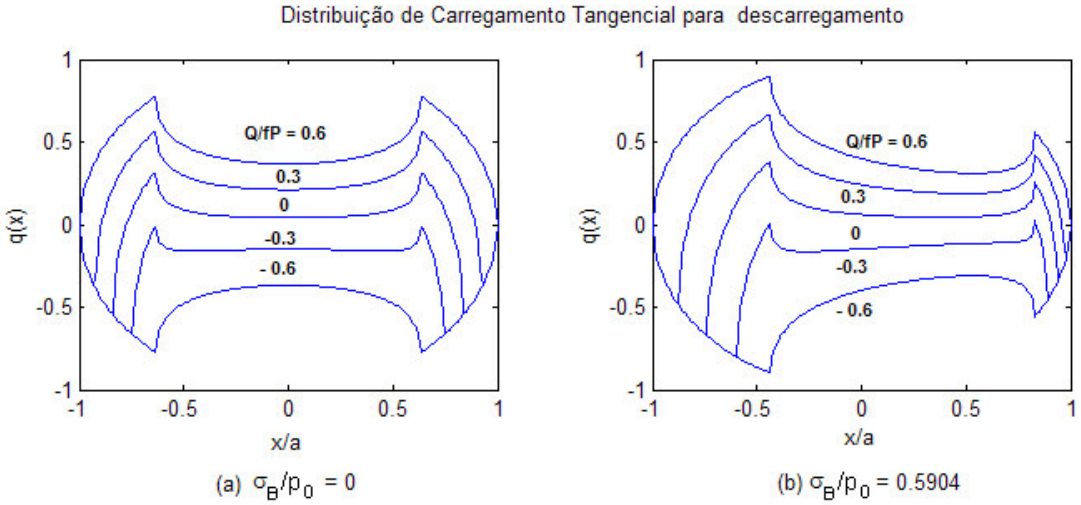

Figure 4: (a) Variation of shear tractions at different instants of the fully reversed fretting cycle. Q/fP varying from +0.6 to –0.6, (b) Effect of the bulk load on the shear tractions shown in (a) for σ_B/p_0 varying from 0.59 a –0.59.

2.2. Surface Stress Field

Returning to the evaluation of the subsurface stress field, it can be obtained, as in the case for monotonic loading, by superposition of the results for the elliptical tractions, although the shifted origins of the perturbation terms, $q'(x)$ and $q''(x)$, will have to be taken in account. It is particularly worthy of note that four different combinations of superposition will be necessary to express the

stress field at maximum and minimum load and during unloading and reloading. For instance, the normalised *xx* component of stress at each of these stages will be:

At maximum (combination + e -) or minimum (- e +) load:

$$\frac{\sigma_{xx}(x,y)}{p_0} = \left(\frac{\sigma_{xx}^{n}\left(\frac{x}{a},\frac{y}{a}\right)}{p_0} \right) \pm f \left(\frac{\sigma_{xx}^{t}\left(\frac{x}{a},\frac{y}{a}\right)}{fp_0} \right) \mp f\frac{c}{a} \left(\frac{\sigma_{xx}^{t}\left(\frac{x-e}{c},\frac{y}{c}\right)}{fp_0} \right) + \sigma_B \tag{20}$$

During loading (combination + , – e +) or unloading (- , + e -):

$$\frac{\sigma_{xx}(x,y)}{p_0} = \left(\frac{\sigma_{xx}^{n}\left(\frac{x}{a},\frac{y}{a}\right)}{p_0} \right) \pm f \left(\frac{\sigma_{xx}^{t}\left(\frac{x}{a},\frac{y}{a}\right)}{fp_0} \right) \mp 2f\frac{d}{a} \left(\frac{\sigma_{xx}^{t}\left(\frac{x-e'}{d},\frac{y}{d}\right)}{fp_0} \right) \pm f\frac{c}{a} \left(\frac{\sigma_{xx}^{t}\left(\frac{x-e}{c},\frac{y}{c}\right)}{fp_0} \right) + \sigma_B(t) \tag{21}$$

where the superscripts n and t stand for the stress components due to the normal and tangential loads respectively. Similar formulation can be derived for the *yy* and *xy* components of stress at these same loading stages, being the *zz* component obtained from the other two direct stresses (plane strain condition). The functions in brackets may be evaluated using Muskhelishivili's potentials (Muskhelishivili, 1953, Hills et al., 1993).

3. RESULTS

The application of methodologies to predict the fretting fatigue strength of mechanical components is usually based on the determination of the subsurface stress field. In this setting, it is of most importance to map such stress field and understand the role of the bulk fatigue stress, σ_B, over it. In the following sections a series of graphs mapping the subsurface stress field for the contact configuration depicted in fig. (2) is presented. The data considered to extract these results were: friction coefficient $f=0.75$, Poisson coefficient $\mu=0.33$, $Q_{max}/fp_0=0.6$ and $\sigma_B^{max}/p_0=0.59$.

3.1. Stress distribution along the contact surface

In this section the distribution of stresses along the contact surface with and without the presence of the bulk fatigue load is presented. Figure (5) shows the variation of the normalized σ_{xx} and τ_{xy}, stress components at the surface ($y/a = 0$) for x/a varying from –2 to +2. The σ_{xx} stress component was calculated at two different instants of the Q load. In Fig 5(a) its variation is depicted for $Q=Q_{max}$ while Fig (5)b corresponds to values at $Q=-Q_{max}$. For all graphs shown from now on dashed lines are used to plot the results obtained when the bulk load is applied (always in phase with the Q load). It seems clear from these graphs that the *xx* component of stress reaches its maximum tensile value at the trailing edge of the contact ($x/a=-1$) and at $Q=Qmax$ (to reach this conclusion different load steps were analysed and space only preclude us to show them all here). Further, its value may be sensibly raised by the presence of the bulk stress.

Figs. 5(c) present the shear traction (τ_{xy}) distribution at $Q=Q_{max}$ and for $\sigma_B=0$ and $\sigma_B\neq0$. It can be noted that the bulk stress cause an visible effect on the shear tractions, which is responsible for the offset in the stick zone, as previously mentioned in this article.

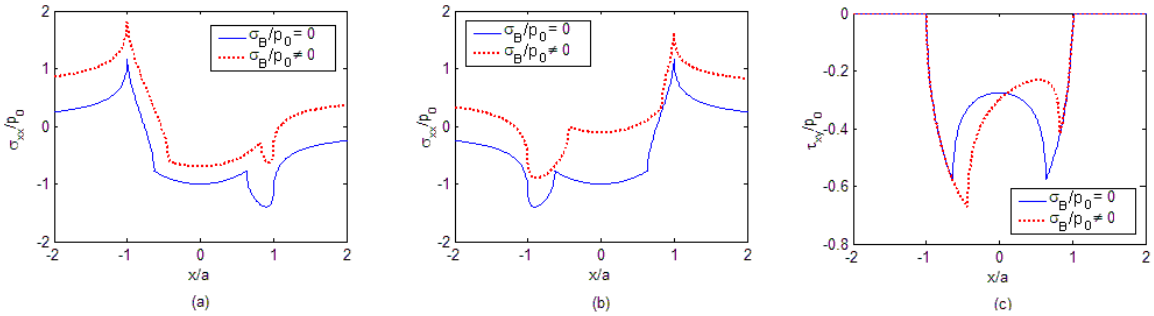

Figure 5: Distribution of different stress components along the contact surface: (a) σ_{xx} at $Q=Q_{max}$, (b) σ_{xx} at $Q= -Q_{max}$, (c) shear tractions τ_{xy} at $Q=Q_{max}$.

3.2. Stress gradient at the trailing edge of the contact

Fretting cracks have shown to nucleate at the trailing edge of the contact for tests carried out under the same configuration analysed in this work (Araújo, 2000). Moreover a number of researchers have pointed out that, in fretting fatigue the stress gradient plays an importatn role on the initiation and early propagation stages of the crack (Araújo, 2000). Hence, the variation of the stress components with depth at this point should be an important aspect to be considered. In this setting, Fig. (6) presents the variation of the σ_{xx}, σ_{yy}, σ_{zz} and τ_{xy} components in the y direction for Q_{max} / fp_0 and at *x/a = -1*. Again the influence of the bulk stress is analysed, being the results with zero bulk stress shown in solid lines and for non-zero bulk stress in dashed ones.

Fig (6)a shows the σ_{xx} stress gradient in the *y* direction. It is worthy of note that σ_{xx} is tensile at the surface but it drops very quickly with depth, becoming compressive for the loadings here considered and in the absence of the bulk stress, whose effect is to shift the whole curve by a constant amount for the tensile side. The σ_{yy} component (Fig. (6)b) is null at the surface and compressive inside the body. There is a small influence of the bulk stress on it, due to the offset of the stick zone, which will change the contribution of *yy* stresses caused by the shear tractions. The τ_{xy} stress (Fig. (6)d) is also null at the surface but it abruptlly changes from positive to negative values in a very short distance from the surface. The variation of the *zz* component with depth is shown in Fig (6)c. As it is a plane strain problem its variation is dependent on the behaviour of the other two direct stress components.

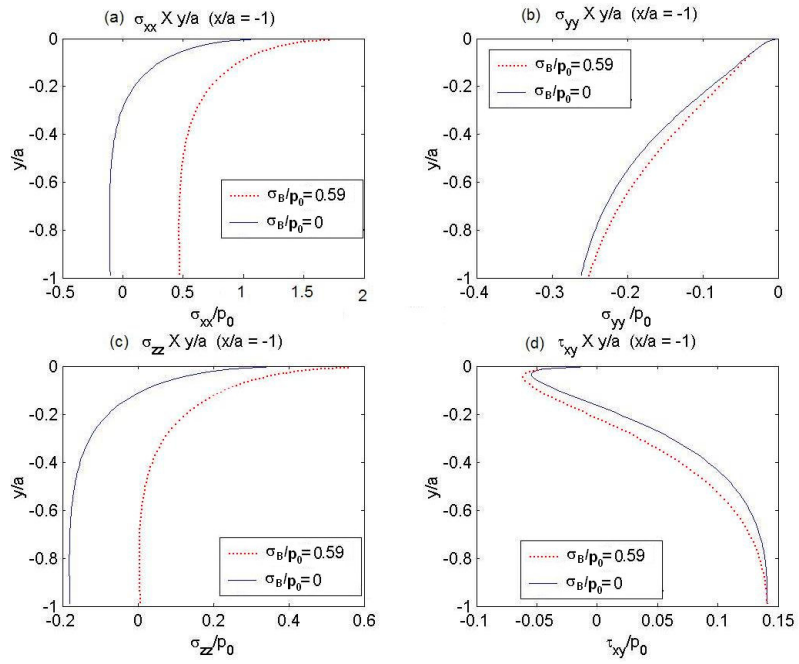

Figure 6: Stress gradient with and without the bulk stress presence for $Q_{max} / fp_0 = 0.6$ and *x/a = -1*: (a) σ_{xx}/p_o X *y/a,* (b) σ_{yy}/p_o X *y/a*, (c) σ_{zz}/p_o X *y/a*, (d) τ_{xy}/p_o X *y/a.*

3.3. Phase diagrams

Phase diagrams of the σ_{xx}, σ_{yy}, σ_{zz} and τ_{xy} stress components were plotted on and under the surface at the trailing edge of the contact to evaluate the stress history (Figs. (7) and (8)) during a loading cycle. To generate these graphs a sinusoidal fully reversed shear load, *Q/fP*, whose amplitude was 0.6 was applied in sixteen time steps (Figs. 7(a) and 8(a)). The effect of the bulk stress is assessed considering it varies in phase with the shear load from +0.5904 to –0.5904. The phase diagrams on the contact surface (Fig.7 (a,b)) show that only the *xx* component of stresss varies in time, hence the problem at this position can be analyzed like a uniaxial case to both zero and non-zero bulk stress. The effect of the bulk stress in this case was to increase the amplitude of variation of the σ_{xx} stress. However, this behaviour changes completely just underneath the contact. At position (*x/a,y/a*)=(-1,0.1) the phase diagrams were assessed again (Fig. (8)), and it is apparent that the stress history becomes a multiaxial one. The bulk stress tends to stretch the phase diagram in he σ_{xx} stress direction always that it is plotted against any of the other stress components.

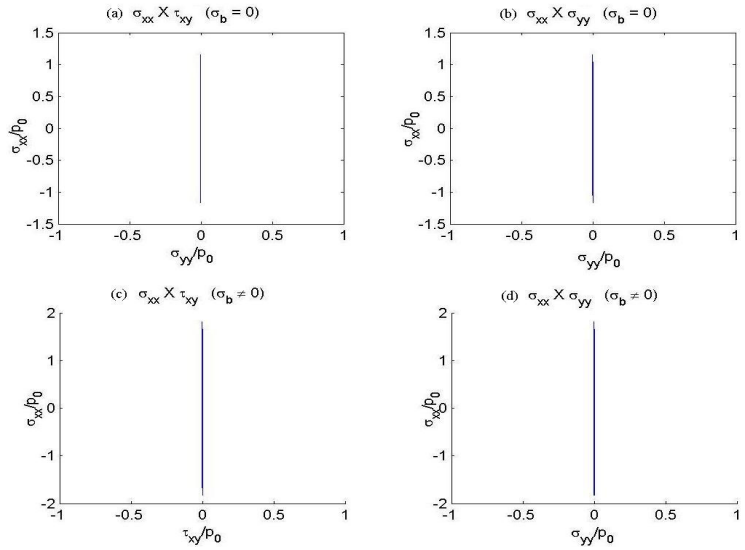

Figure 7: Phase diagrams at (x/a, y/a) = (-1, 0) for *Q/fP* varying from 0.6 to –0.6 to σ_{xx} X τ_{xy}, σ_{xx} X σ_{yy} for σ_B/p_0=0:(a)-(b), and for σ_B/p_0=0.5904: (c)-(d). σ_{yy} X τ_{xy} gives only a point at (0,0).

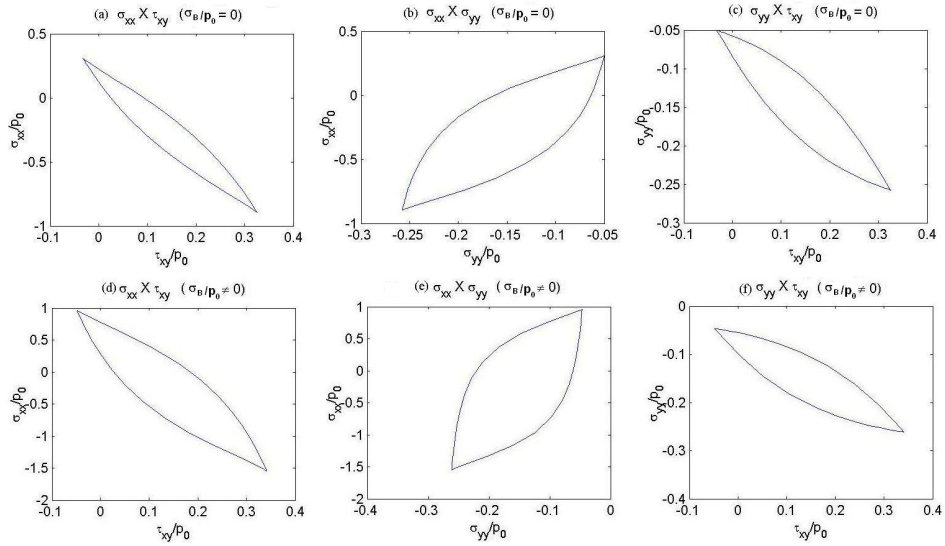

Figure 8: Phase diagram at (*x/a, y/a*)=(-1, 0.1) for *Q/fP* varying from 0.6 to –0.6 to σ_{xx} X τ_{xy}, σ_{xx} X σ_{yy}, σ_{yy} X τ_{xy} for σ_B/p_0=0: (a)-(c) and for σ_B/p_0=0.5904: (d)-(f).

4. CONCLUSION

This work conducted a detailed analysis of the stress field produced in a contact configuration often used in fretting fatigue tests. More specifically we investigated the effects of the bulk stress on the stress field produced by the contact of cylinders under a partial slip regime. It was shown that the bulk stress provokes an offset of the stick zone, which changes the shear traction distribution, however it has no effect on the pressure. On the contact surface the xx component of stress reaches its highest value at the trailing edge of the contact, when *Q/fp=Qmax*. Further its value is significantly higher than the value reached by the other stress components in any other position on the surface and at any other instant. At this time, one should remember that the xx stress is

responsible for Mode I cracking, and that experimental work considering this same contact configuration has shown that fretting cracks usually have nucleated at this position. The presence of the bulk stress increased the severity of the xx component of stress at all surface points.

An analysis of the variation of the stresses against depth at the trailing edge of the contact showed that all components experiment a severe stress gradient. The σ_{xx} stress reached the highest tensile values at the surface but dropped very quickly at a short distance from the surface becoming compressive at a certain stage. The bulk stress further increased its severity on the surface and avoided it dropped to compressive values at any depth. The other stress components hardly felt the effect of the bulk stress in this analysis.

At last a phase diagram assessment proved that the state of stress is uniaxial at the trailing edge of the contact, being σ_{xx} the only non zero stress. Superposition of the bulk stress was responsible for a significant increase in its amplitude. On the other hand the phase diagrams showed there is a multiaxial state of stress just underneath the contact surface.

5. ACKNOWLEGMENTS

The authors would like to acknowledge the financial and technical support of the Superintendência de Expansão e Geração of Eletronorte SA. The CNPq IC scholarship is gratefully acknowledged.

6. REFERENCES

Araújo, J.A. (2000), "On the initiation and arrest of fretting fatigue cracks", D. Phil thesis, Oxford, 2000.

Eden, E. M., Rose, W. N., and Cunningham, F. L. (1911), Endurance of Metals, *Proceedings of the Institute of Mechanical Engineers*, Vol.4, pp.839-974.

Fuenmayor, J., Ródenas, J.J. and Tur, M. (2003), "Influence of Bulk Stress on Contact Conditions and Stresses During Fretting Fatigue", Journal of Strain Analysis, Vol. 37, No. 6, pp. 479-492.

Hertz, H. (1882), Uber die Beruhrung fester elastischer Korper, *Jnl. Reine und angewandte Mathematik*, 92, pp. 156-171.

Hills, D. A., Nowell, D. and Sackfield, A. (1993), *Mechanics of Elastic Contacts*, Butterworth-Heinemann Ltd.

Mindlin, R. D. (1949), Compliance of elastic bodies in contact, *Jnl. App. Mech.*, 16, pp. 259-268.

Muskhelishvili, N. I. (1953), *Some Basic Problems of Mathematical Theory of Elasticity*, Noordhoff, Gröningen.

Nowell, D., and Dai, D.N. (1998), Analysis of surface tractions in complex fretting fatigue cycles using quadratic programming. *ASME Jounal of Tribology*, 120, pp. 744-749.

Warlow-Davies, F. J. (1941), Fretting Corrosion and Fatigue Strength, *Proceedings of the Institute of Mechanical Engineers*, Vol.146, pp.32.